Surface-Enhanced Raman Spectroscopy Studies on the Adsorption and Electrooxidation of Carbon Monoxide at the Platinum−Formic Acid Interface

Peigen Cao,*,† Yuhua Sun, and Renao Gu*

Department of Chemistry & Chemical Engineering, Suzhou University, Suzhou 215006, P. R. China

Received: May 14, 2003; In Final Form: January 29, 2004

The vibrational spectrum of carbon monoxide, exerted by dissociation of formic aid, has been investigated at the platinum electrode as a function of applied potential by using the surface-enhanced Raman spectroscopy (SERS) technique. The electrolyte is 0.1 M $LiClO_4$. Two typical SERS features observed at 475−490 and 2055−2080 cm^{-1} are attributed to the platinum−CO (ν_{Pt-C}) and intramolecular C−O (ν_{C-O}) stretching vibration, respectively, indicating linearly adsorbed CO on platinum. Comparisons of the present data with previous studies in aqueous solutions show that solution components, particularly the dielectric in the inner double layer, may significantly influence the interaction of CO with platinum, especially the CO intramolecular mode. Electrooxidation of CO was observed to occur at potentials more positive than 0.6 V, being slightly negative relative to previous studies for CO on smooth platinum, suggestive of a higher electrocatalytic activity for the present highly roughened platinum surface. At positive and moderately negative potentials (−0.2 to 0.6 V), the Pt−C and CO intramolecular bands exhibit opposite frequency changes with decreasing potential, with Stark tuning rate being −6 and 24 cm^{-1}/V, respectively. At more negative potentials, both ν_{Pt-C} and ν_{CO} exhibit nonmonotonic potential dependences. The gradually decreasing slope for ν_{Pt-C} can be explained in terms of the nearly offsetting contributions from the π-back-donation and σ-bonding, along with increasing steric repulsion from negatively charged surfaces. The nearly potential-invariant frequencies for ν_{CO} were observed at potentials more negative than −1.0 V, indicating the key role of increasing concentration of H^+ in the inner double layer, possibly weakening the electron density back-donated from platinum to CO $2\pi^*$ orbitals.

Introduction

The adsorption and electrooxidation of carbon monoxide on metal surfaces have been investigated extensively in aqueous solutions[1−5] as well as in ultrahigh vacuum (UHV)[6−8] in the literature. This is mainly due to the following two reasons. First, there is fundamental interest in unraveling the nature of interaction of carbon monoxide with metal surfaces, for CO being a model adsorbate at the metal−solution interface, and bonding of CO to the surface being largely sensitive to the chemical, geometric, and electrostatic environment, as reflected most commonly in the chemisorbate vibrational properties. Second, this molecule has long been regarded as the poisoning intermediate during the direct electrooxidation of methanol and formic acid on platinum or its alloys as catalysts. Understanding the interaction of carbon monoxide with metal surfaces would be expected to shed light into both the electrooxidation mechanism of the C_1 fuel like methanol, formic acid, etc., on platinum and the development of the studies of direct methanol/formic acid fuel cells.

Before the 1980s, most investigations along these lines have been performed by using classical electrochemical techniques, from which a wealth of kinetic and also macroscopic information has been obtained. However, these methods suffer from a lack of molecular-level description of the solid−liquid interface. With the development of infrared (IR) and sum frequency generation (SFG) techniques applicable to electrochemical environments at the beginning of the 1980s, in situ vibrational spectroscopy of CO at platinum electrodes has been obtained and has attracted considerable attention.[3,5,9−13] Of particular interest and much-discussed feature is the significant and even substantial dependence of the intramolecular CO frequencies (ν_{CO}) upon the applied electrode potential, which is generically termed the "Stark tuning effect".[14] On the basis of the IR observations and related theoretical calculations, this effect has been explained in two different ways: as a change in the molecule's chemical bonding and as the effect of electric field in the double layer on the molecule, i.e., the vibrational Stark effect. Combination of such "chemical bonding" and "electrostatic field" has also been proposed in the literature as a complete description of "electronic polarization".[15] Consequently, controversy still exists as regards the nature of the interaction of carbon monoxide with metal surfaces as well as its changes upon the external applied potential.

The third in situ vibrational technique, also applicable to electrochemical environment, is surface-enhanced Raman spectroscopy (SERS).[16] The major features of SERS, especially in comparison with IR and SFG, consist of a much wider detectable band frequency range, in particular the relatively high sensitivity in the low-wavenumber range (below 800 cm^{-1}). This allows for the possibility of direct observation of the metal−adsorbate interaction (for CO, the ν_{m-C} band). However, the observation of enormous (10^6-fold or greater) Raman scattering enhancements for species at roughened metal surfaces is limited for most practical purposes to the coinage metals copper, silver,

* Corresponding authors. E-mail peigen@caltech.edu, ragu@suga.edu.cn.

† Present address: Division of Chemistry & Chemical Engineering, m/c 127-72, California Institute of Technology, 1200 E. California Blvd., Pasadena, CA 91125.

10.1021/jp035324z CCC: $27.50
Published on Web 03/23/2004

and gold. Of particular interest and importance is to extend this enhancement effect to other transition metals such as Pt-group metals, which are used as catalysts in many technologically important processes. Weaver and co-workers[17] used a deposition method to prepare the platinum-coated gold electrode, which exhibited well-resolved SERS spectra of adsorbed carbon monoxide via the electromagnetic long-range effect of the SERS-active substrate gold. Recently, this deposition procedure has been developed, and they claimed that the pinhole-free ultrathin film of platinum coated onto gold, yielding optimal SERS properties with little or no chemical/spectral interferences from the underlying gold substrate, can be readily obtained.[18]

Recent studies by Tian and co-workers along these lines have found that the surface enhancement factor (SEF) of Raman scattering for other transition metals (Pt, Ru, Rh, Pd, Fe, Co, Ni, and their alloys), albeit small in comparison with the above three coinage metals, indeed exists, and the SEF value varies from 10-fold to 10^3-fold depending on the nature of the metal and the proper surface roughening procedures.[19−21] Several typical organic or inorganic adsorbates adsorbed onto the highly roughened platinum electrodes from aqueous solutions have been examined, and particularly useful information reflecting the metal−adsorbate interaction can be well resolved, enabling further probing of the nature of the molecule−platinum surface interaction occurring in the electrochemical system.

In the present paper, the recently discovered transition metal SERS effect has been utilized to probe the potential-dependent vibrational properties of adsorbed carbon monoxide, exerted from dissociation adsorption of pure formic acid as solvent on platinum. This is initially prompted by recent success in our laboratory in observing well-resolved Raman spectrum of pyridine on platinum in nonaqueous acetonitrile solution.[22] The interference of the signal from organic solvents can be substantially removed by using both the confocal microprobe lens system and proper activation procedure on platinum, yielding SERS-active Pt surfaces. The motivation for the choice of the Pt/CO system in nonaqueous formic acid solution is also based on the following several reasons. First, most of the investigations as regards the electrochemical Pt/CO system were performed in aqueous solutions according to the literature.[23−25] Only a few papers were concerned with vibrational spectra of carbon monoxide in the presence of nonaqueous solvent partly due to the relatively low solubility of CO in these aprotic solvents.[23] However, the advantage of using organic solvent over aqueous solutions is also evident that it can extend widely the potential region where adsorption process occurs. While in aqueous systems, the availability of potential region is largely limited by the hydrogen evolution reaction at negative potentials and oxidation of carbon monoxide to carbon dioxide at relatively positive potentials. Second, much attention has been focused on the vibrational properties of C−O stretch mode for this archetypal electrochemical system due to the unavailability of detection of low-frequency bands by using the IR or SFG technique. Bearing in mind that the application of SERS on this system would make it possible to obtain directly metal−chemisorbate vibration, the present investigation by using this technique would be expected to shed light or at least provide further key information on the nature of the interaction of CO with metal surfaces, particularly the field-dependent binding of CO with the surface. Finally, the widely used metal substrate for this typical Pt/CO system contains mainly single crystalline Pt(*ijk*), which facilitates the comparisons between data obtained from electrochemical and UHV environments. These smooth platinum surfaces are completely different from the highly roughened materials used in practice. However, the preparation of the latter surface is exactly the prerequisite to obtain SERS effect of Pt, which on the contrary facilitates investigations on the surface chemical bonding at such highly roughened metal surfaces. Hence, studies along these lines may provide a way to bridge the gap between the systems of fundamental research and practical applications.

Experimental Section

Materials. The solvent, formic acid (99.5%), was of analytical reagent and used without further purification. The SERS measurements were made in 0.1 M $LiClO_4$/formic acid solutions at room temperature. The anhydrous salt used in this work, lithium perchlorate (analytical reagent grade), was dried by heating under vacuum up to 60 °C for 6 h before use. The chemical used for activating the platinum surface, sulfuric acid, was also of analytical reagent. The solution used for roughening the platinum surface was 0.5 M H_2SO_4, prepared by using distilled Milli-Q water.

Electrochemical Roughening Procedures. Electrochemical roughening of the platinum electrode was performed in a three-compartment electrochemical cell. The working electrode was a polycrystalline Pt (99.99%) rod embedded in a Teflon sheath, with a geometric surface area of 0.1 cm^2. A large Pt ring and a saturated calomel electrode (SCE) were served as the counter and reference electrodes, respectively. All the potentials, unless specified, are reported vs the SCE electrode. An EG&G model 173 potentiostat was employed to control the applied potentials. Briefly, the roughening procedure contains mechanically polishing of the Pt electrode successively with 0.5 μm aluminum powder down to 0.05 μm until that a mirror finish of the surface was obtained. This was followed by ultrasonic cleaning with Milli-Q water. Then, a square wave of 1.5 kHz with upper and lower potentials of 2.4 and −0.2 V was applied to the electrode in 0.5 M H_2SO_4 for 5−10 min. The potential was then polarized at −0.2 V until the electroreduction of the surface Pt oxides was completed. An additional potential cycle between −0.3 and 1.25 V at a scan rate of 500 mV/s was employed to the electrode in order to remove the unstable atoms or clusters, which then yielded a stable Pt surface for the acquisition of the SERS spectra. The roughened Pt electrode was then immersed in formic acid and rinsed by the solvent before use in order to eliminate contamination of water.

Raman Measurements. The spectroelectrochemical cell used for in situ Raman measurements was similar to that used for the roughening of platinum except that the cell was dried in a vacuum oven at 120 °C before use. In addition, there is a transparent glass window attached to the top of the cell to decrease the contamination of water during SERS measurements. SERS data were obtained using a confocal microprobe Raman system (LabRam I from Dilor, France). The excitation wavelength was 632.8 nm from an inner air-cooled He−Ne laser with a power of 10 mW and a spot of size 3 μm at the sample surface. The slit and pinhole used were 200 μm and 800 μm, respectively. The acquisition time was 100 s, and the accumulation was 4 times for each spectrum. With a holographic notch filter and a CCD detector, the spectrometer has an extremely high detecting sensitivity. A 50× long working distance objective (8 mm) was used so that it was not necessary for the objective to be immersed in solution. This is key important for both the requirement of in situ measurements and the decrease or even substantial elimination of the interference from the signal of bulk organic solvents. A more detailed description of Raman measurements can be found elsewhere.[2b]

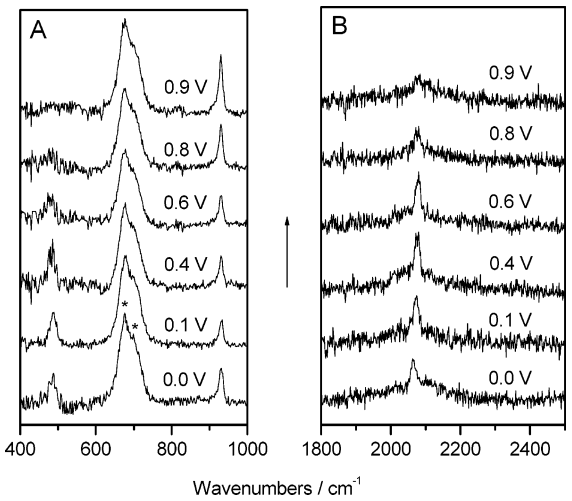

Figure 1. Representative potential-dependent surface Raman spectra from a roughened platinum electrode in 0.1 M $LiClO_4$/formic acid within the low- and high-frequency regions: (A) 400−1000, (B) 1800−2500 cm^{-1}. The potential region is from 0.0 to 0.9 V. Laser line: 632.8 nm; acquisition time: 100 s; accumulations: 4.

Results

Figure 1A,B shows a typical set of potential-dependent SER spectra from a roughened platinum electrode in formic acid containing 0.1 M $LiClO_4$. The spectrum is presented in the low and higher frequency regions covering the Pt−C (ν_{Pt-C}) and C−O (ν_{C-O}) vibrational modes: 400−1000 and 1800−2500 cm^{-1}. The starting acquisition potential is 0.0 V, exactly approaching the open-circuit potential of the system. Then the electrode potential is altered to positive values in a staircase fashion, usually in 0.1−0.2 V increments.

The spectral features presented in Figure 1 suggest dissociative chemisorption of formic acid to yield carbon monoxide. This is clearly evident for the appearance of both ν_{Pt-C} and intramolecular ν_{C-O} vibrational modes, located at 475−490 and 2055−2080 cm^{-1}, respectively. The present observation of dissociative chemisorption of formic acid on platinum is consistent with previous studies on smooth platinum examined by IR and SFG techniques.[26−28] The resulting carbon monoxide is generally designated to the so-called poisoning intermediate, which adsorbs strongly onto the Pt surface inhibiting further oxidation of formic acid. The detection of reaction intermediates at the present nonaqueous interface is helpful to examination of the mechanism of electrooxidation of formic acid. This issue will be discussed further elsewhere.[29] Here we focus attention on the spectral behavior and corresponding environmental effects, in particular the external electric field on the chemisorption of CO at the Pt/formic acid interface.

A noteworthy point here is the ability to observe the high-quality surface Raman spectrum of a CO adlayer on Pt, in particular the low-frequency component reflecting Pt−CO interactions, usually inaccessible to infrared spectroscopy. Although SER spectra of carbon monoxide formed from dissociation of formic acid were obtained recently by Weaver and co-workers[30] on a rhodium/platinum film electrode (deposited on gold), the deposition film may not be unique, and the possible existence of pinholes in the film may inevitably bring about some ambiguities to the explanations of spectra. The better method is to obtain SER spectra of CO from bare platinum electrodes. To the best of our knowledge, it may be the first time in this paper to record the nonaqueous SER spectra of carbon monoxide exerted by dissociation of formic acid on bare platinum surfaces over a wide potential range. This is mainly due to the combination of the roughening pretreatment on Pt electrodes and the application of confocal optical configuration. This enables substantial elimination of the interference of a strong Raman signal from bulk solution phase, which is rather serious in the case of nonaqueous solvents. In addition, roughening of the Pt electrode also generated a SERS-active surface, with surface enhancement factor (SEF) being an order of ca. 10^2, which makes possible the observation of Raman spectrum of CO featuring small scattering cross section. The detailed discussion of SEF calculations and SERS mechanisms for transition metals can be found in ref 31.

Considering first the low-frequency data (Figure 1A), the bands marked with asterisk are readily designated to modes of the bulk solvent formic acid. Another band observed at 933 cm^{-1} corresponds to the totally symmetric stretch of perchlorate anion. The most striking feature is the observation of a new band evident at 486 cm^{-1} (0.0 V, Figure 1A) compared with the normal Raman spectrum of formic acid solution. The corresponding frequency shifts to lower values with increasing positive potentials. This band is readily assigned to the ν_{Pt-C} mode, consistent with the SERS result of CO at Pt-coated gold electrodes[32] as well as electron energy loss spectra (EELS) obtained from the Pt(111)/CO system under ultrahigh vacuum.[33] As the potential is altered to a more positive value than 0.8 V, the Pt−C band decreases rapidly in intensity, indicating the initiation of electrooxidation of CO on Pt. The slight change of intensity of the ClO_4^- band may be reflective of its quantity change in the vicinity of the electrode surface induced by variations of electric field in the double-layer region.

The high-frequency spectra display a clear feature at 2055−2080 cm^{-1}, which can be readily identified as arising from linearly-bonded (or atop) CO on Pt. In contradiction with ν_{Pt-C}, this band blue-shifts upon scanning potential to more positive values as is normally observed for atop CO. The identification of a rather weak feature located at ca. 2000 cm^{-1} as a shoulder of atop CO band is largely obscure. Although the frequency value approaches that (1650−2000 cm^{-1}) normally observed for bridgely bonded (or 2-fold bridging) CO on platinum-group metals,[34] the assignment of this band to bridging CO is somewhat risky. In addition, the absence of the corresponding ν_{Pt-C} mode, usually observed at 380−440 cm^{-1} for bridgely bonded CO,[14d,35] may not support the presence of bridging CO. Thus, the present observation of predominant atop CO on platinum is in agreement with the quantum-chemical rationale for the increasing preference for atop vs multifold CO coordination observed in the series Pd < Pt ∼ Rh < Ir ∼ Ru.[5] As the potential is moved to more positive values than 0.8 V, the intensity of the C−O mode decreases, consistent with changes in ν_{Pt-C}, indicative of CO oxidation. More interestingly, the frequency of the C−O band also decreases at largely positive potentials. This phenomenon is also observed in aqueous solution by IR techniques[36] and will be analyzed further below.

For a better understanding of the chemisorption behavior of CO on platinum over a wider potential range, the spectral sequences for CO adlayers on Pt were also acquired upon scanning potential back to negative values. Figure 2A,B displays such a set of potential-dependent SER spectra at 0.0 to −2.0 V. Similarly to the positive potential region, CO features are clearly evident even at largely negative potentials (for instance, −2.0 V). In combination with spectral features in Figure 1, spectrum of CO adlayer could almost be observed in a wide potential range (∼3 V). This is inaccessible to aqueous solution, where the typical spectral window is about 0.5 and 1.0 V for acid and alkaline solutions, respectively, due to the bound by

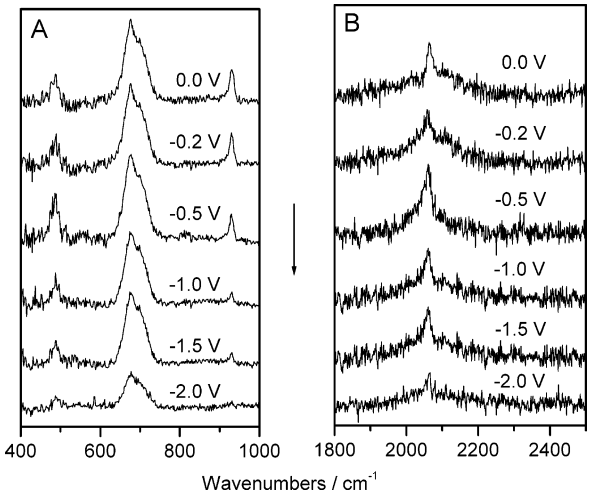

Figure 2. As for Figure 1, but the potential region is from 0.0 to −2.0 V.

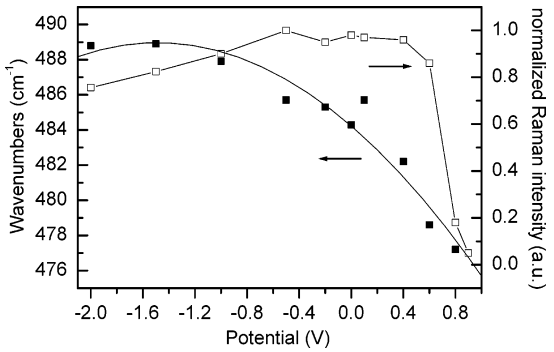

Figure 3. Dependence of the frequency and integrated band intensity vs applied potential for ν_{Pt-C}. The polynomial fit of the frequency data is shown as line.

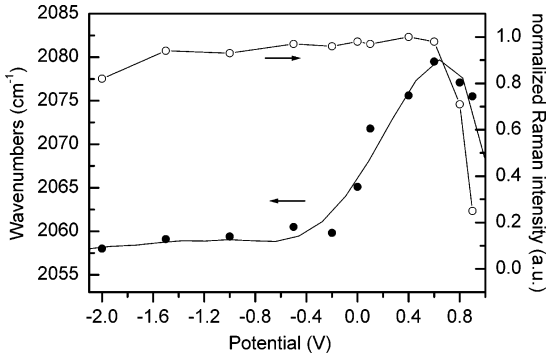

Figure 4. As for Figure 3, but for the CO intramolecular band.

oxidation of CO to carbon dioxide at positive potentials and desorption of CO to allow hydrogen evolution at negative potentials. This again shows a major advantage of organic solutions for studying potential effects on the properties of surface species spectra.

The comparative examination of the SERS $\nu_{Pt-C}-E$ and $\nu_{CO}-E$ dependencies observed for platinum is of central interest here. For the purpose of convenient discussion, taken from SERS data in Figures 1 and 2, the peak intensities and frequencies of the Pt−CO and atop C−O stretches are plotted respectively vs the electrode potential (see Figures 3 and 4). Note that the integrated peak intensity was first divided by that of the solvent band (marked with asterisk, taken as a standard) and then normalized to the corresponding maximum band intensity. Because of the influencing effect of CO coverage on frequencies of the ν_{Pt-C} and ν_{CO} bands, discussions on the frequency dependencies will be limited to the potential region where both CO electrooxidation and hydrogen evolution reaction would not occur, typically at −1.6 to 0.6 V (see Figures 3 and 4). Note that the relatively weaker solvent band observed at potentials negative to −1.6 V (Figure 2A) is likely to be caused by the hydrogen bubbling. In addition, the decreasing band of ClO_4^- stretch in intensity toward more negative potentials may be attributed to both the interference of hydrogen bubbling and strong electrostatic repulsion from the largely negative charged surface.

The most striking features here in Figures 3 and 4 may be the observation of nonlinear potential dependencies of the Pt−C and C−O bands. Further inspection of these vibrational frequency−potential data reveals several significant features. First the ν_{Pt-C} slopes, $d\nu_{Pt-C}/dE$, are calculated to be −6 cm^{-1}/V over the potential region −0.2 to 0.6 V accessed also by studies in aqueous solutions. This is in agreement with previous reports from terminal CO SERS features on Pt electrodes in acid and/or alkaline aqueous solutions ($d\nu_{Pt-C}/dE = 4-5$ cm^{-1}/V).[35] A slight higher absolute value of 10−20 cm^{-1}/V was observed by Weaver and co-workers.[14d] This may be caused by the use of Pt film electrodes in their study, which exhibits minor differences in the surface microscopic structure and related electronic properties in comparison with bulk platinum substrates. In fact, a corresponding larger full width at half-maximum (fwhm 50 cm^{-1}) for the C−O bands was also observed from Pt-film electrodes,[14d,17] when compared with the present data (fwhm 20 cm^{-1}). More interestingly, as seen from Figure 3, the Pt−C mode becomes gradually independent in frequency upon scanning potential to largely negative values (typically < −1.4 V). The polynomial fit of the experimental frequency data (shown also in Figure 3 as a line) even gives a maximum frequency value at −1.5 V. This surprising observation is not reported in the literature up to now. It may be due partly to the inaccessible largely negative potential regions in previous SERS studies at the Pt/aqueous interface. However, the present striking findings are in good agreement with recent quantum chemical calculations for the Pt/CO system by using density-functional theory (DFT).[5] A detailed discussion will be given in a later part of this paper.

Second, the Stark tuning rate for intramolecular CO vibration at potential region −0.2 to 0.6 V is anticipated to be 24 cm^{-1}/V, which is comparable to previous IR results (15−25 cm^{-1}/V) obtained from nonaqueous solutions.[24,25,37] This is considerably less than that observed in aqueous systems (30 cm^{-1}/V) and is possibly due to the different dielectric constant of nonaqueous solvents compared with water, which causes a smaller potential drop across CO adlayers on platinum. Additionally, the slope of the $\nu_{CO}-E$ plot decreases quickly as the potential is moved to more negative potential regions (see Figure 4), almost approaching zero upon moving potentials more negative than −1.0 V. A possible explanation for this is that no change of potential across the interface would occur due to the large ohmic drop in the bulk solution. However, the frequency behavior for ν_{CO} was still observed when increasing the concentration of the electrolyte. The large current observed at negative potentials in the cyclic voltammogram may be due to the use of "absolute" formic acid. In addition, if the possibility that no interfacial potential change would occur was considered, both the ν_{CO} and ν_{Pt-C} would be expected to exhibit no frequency change upon potential. This is not consistent with the experimental observations. Subsequently, the above phenomenon may be indicative of significant structural changes in

TABLE 1: Comparison of the Typical Frequency Data and Corresponding Stark Tuning Rates of the ν_{Pt-C} and ν_{Pt-C} Vibration for Various Aqueous and Nonaqueous System.

	system	techniques	ν_{Pt-C} (cm^{-1})	$d\nu_{Pt-C}/dE$ (cm^{-1}/V)	ν_{C-O} (cm^{-1})	$d\nu_{C-O}/dE$ (cm^{-1}/V)	potential range (V)	reference
nonaqueous	Pt(smooth)−acetonitrile	IR			2040−2095	15−24	−2.0 to 1.0	24, 25, 37c
	Pt(smooth)−methanol	IR			2055−2090	20−25	−0.9 to 0.8	25, 37b
	present	SERS	475−490	6 (−0.2 to 0.6 V)	2055−2080	24 (−0.2 to 0.6 V)	−1.6 to 0.6	
aqueous	Pt(smooth)−acid aq	IR			2050−2070	∼30	0.0 to 0.5	3, 36
	Pt(smooth)−alkaline aq	IR			∼2020			40
	Pt(film)−acid aq	SERS	460−465	10−20	2055−2075	∼30−40	−0.2 to 0.4	14d, 17
	Pt(film)−alkaline aq	SERS	468−475	10−20	2010−2050	∼40−60	−0.8 to −0.2	14d, 17
	Pt(rough)−acid aq	SERS	485−490	4−5	2065−2075	26	−0.2 to 0.2	2, 35
	Pt(rough)−alkaline aq	SERS	505−510	∼10	1990−2020	∼40	−1.0 to −0.5	35

the double-layer region, which contradict at least partly to the effects of external negative electric field experienced by CO adlayers.

Discussion

Chemisorption and Electrooxidation of Carbon Monoxide The C-down adsorption model for CO on surfaces is generally assumed for CO adsorbed on transition metals, as derived by the large downshift of vibration of intramolecular CO mode (about 100 and 60 cm^{-1} from "free" and solvated CO molecules, respectively) based on the so-called Blyholder model.[38] It suggests that the bonding between CO and platinum occurs due to a charge transfer from the 5σ orbital of CO to the unoccupied metal orbitals followed by a back-donation from the d_π metal orbitals to the $2\pi^*$ unoccupied level of CO. Accordingly, this is also referred to as the σ donation−π back-donation mechanism.[39] However, the present detection of a low-frequency band at 475−490 cm^{-1} even in nonaqueous media show a more clear evidence for the above-assumed C-ended configuration.

Subsequently, interest arises from the comparison of the present data with previous observations for the archetypal Pt−CO system. We aim to shed light on the understandings of the environmental effects, specifically the solvent types, solution pH, and electrolyte components, etc., on the nature of metal−CO bonding. Listed in Table 1 are the frequency values normally observed for the Pt−C as well as intramolecular CO vibration and the corresponding shifts in frequency upon potential, i.e., Stark tuning rate, in both aqueous and nonaqueous systems. Several significant features can be discerned from Table 1. First, while the present observed Pt−C vibration shows a comparable frequency value with previous reports in aqueous solutions, slight differences can still be found. The bulk platinum gives a relatively higher Pt−C vibration frequency compared with Pt film electrodes in a comparable potential region. Additionally, a slight higher $d\nu_{Pt-C}/dE$ as mentioned above is observed for the latter system. However, a similar $d\nu_{Pt-C}/dE$ exists for roughened bulk platinum electrodes in both aqueous and nonaqueous system. The sensitivity of the Pt−C vibration to the substrate and relatively insensitivity of this bond to electrolyte components may be indicative of the greater effects of the surface microscopic structures and related electronic properties (hence the extent of charge transfer) on the metal−CO interaction. In fact, a large downshift of frequency to about 370 cm^{-1} has ever been observed for CO on palladium electrodes compared with platinum.[14d]

Second, interestingly, the vibration of intramolecular CO bond is more easily affected by the solution components, particularly the electric double-layer structure. This conclusion can be brawn by comparison of data in Table 1. Considering the same solution, similar CO vibration frequencies are found for different Pt surfaces. On the contrary, the alkaline solution presents a rather low ν_{CO} in comparison with acid solutions. Another striking feature found from Table 1 is that a slight lower Stark tuning rate for ν_{C-O} is always observed for nonaqueous media than that for aqueous solutions, regardless of the platinum surfaces used. Several important factors, including electrolyte components, CO surface coverage, and adsorption orientation, etc., have been found to have a great impact on the potential dependencies of CO vibration. For a given system, the Stark tuning rate has been derived theoretically by Lambert:[14a]

$$d\nu/dE = (d\nu/dF)(C/\epsilon) \quad (1)$$

where $d\nu/dE$ is the frequency shift with change in electrode potential, $d\nu/dF$ is the frequency shift with change in the electric field strength, C is the interfacial capacity, and ϵ is the solvent dielectric constant. Therefore, three important factors, $d\nu/dF$, C, and ϵ, will determine the Stark tuning rate. In the case of adsorbed carbon monoxide, the sum of the Pt−C and C≡O bond lengths is anticipated to be about 0.3 nm. It is reasonable to assume that the environmental effects within this 0.3 nm critical region are virtually responsible for change of the CO vibrations. In aqueous systems the large fields (about 10^7 V/cm) across the double layer will force the water dipoles to line up toward the electrode surface, causing the dielectric constant to decrease rapidly from 78 (bulk value) to 6−8. Hence, the penetration of relatively small water molecules into the CO adlayer will inevitably change the corresponding dielectric constant and accordingly influence the potential dependence of CO vibration. On the contrary, most of organic solvents featuring relatively larger volume compared with water will have more difficulty to approach such a 0.3 nm critical region, resulting in apparently different Stark tuning rate. Therefore, the present observation of a slight larger rate (24 cm^{-1}/V) may be indicative of the possible approaching of the hydroxyl function group of formic acid to the vicinity of Pt surfaces.

Comparison of the onset potential of CO electrooxidation with previous IR data will also give interesting results. A slight positive onset potential (0.9 V vs SCE) for CO on platinum in absolute methanol was reported by Mcquillan and co-workers.[40] Studies in acetonitrile by Anderson and Huang[37a] showed that CO oxidation occurred at 1.0−1.5 V (vs SCE), far more positive than the present data. These disparities may originate from the smooth Pt substrate used in IR investigations, while the present roughened Pt surface is known to have many surface defects, resulting in a high electrocatalytic activity. Therefore, the oxidation of carbon monoxide will be relatively unique and easy to perform.

Electric Field Effects on Metal−CO Bonding The most intriguing findings of the present results may be the observation of nonmonotonic field dependences of the ν_{Pt-C} and ν_{CO} vibration. A key question arises accordingly: what is the main reason to cause the nonlinear properties of frequency? For the

present given system, change in the surface coverage and adsorption orientation of CO may not be taken into account at −1.6 to 0.6 V (see Figures 3 and 4), for otherwise significant changes in observation of the Pt−C bond and corresponding band intensity would be expected. Subsequently, the external interfacial field should play a key role in the observed Stark tuning behavior. Take eq 1 again for further consideration. For the simplest approximation, the ratio ϵ/C may be displaced by the effective double-layer thickness, d_i. Accordingly, one can deduce from eq 1 that

$$d\nu/dE = (d\nu/dF)/d_i \quad (2)$$

Then, the Stark tuning rate may be directly related to the $d\nu/dF$ value. One may assume that the tuning slopes may be accounted for essentially in terms of electrostatic field effects. However, the observation of nonmonotonic frequency shifts upon potential seems to suggest that the effect of the interfacial field be not consistent over the whole potential region. In other words, the electric field induced changes on the metal−CO bonding, or chemical effects, may coexist.

Both the electrostatic and chemical effects on the vibrational frequencies of CO were considered by Korzeniewski et al.[41] in a semiclassical analysis of the Pt−CO system. For the former assumption, they predicted that $d\nu_{CO}/dE \approx 9 \times 10^{-7}$ cm^{-1} (V cm^{-1})$^{-1}$. Suppose that the effective inner double-layer thickness d_i is roughly that of the CO adlayer, i.e., 0.3 nm; one can obtain from eq 2 about 30 cm^{-1}/V for $d\nu_{CO}/dE$. This is comparable with the experimental findings, particularly those from aqueous systems. However, the corresponding calculation for $d\nu_{Pt-C}/dE$ (less than 3 cm^{-1}/V) does not match well with experimental observations. On the contrary, the alternative calculation based on the chemical effect assumption yielded an increased $d\nu_{Pt-C}/dE$, which is in good agreement with the present findings. Subsequently, the present observations of the potential-induced ν_{Pt-C} shifts can be explained as follows. The marked increase in ν_{Pt-C} with decreasing electrode potential may be caused by the greater π-back-donation from Pt to CO, as proposed by Head-Gordon and Tully.[42] The back-donation effect would be expected to strengthen the Pt−CO bonding. However, this effect may be offset by the increasing Columbic repulsion from the metal substrate, along with a decreasing σ-donation from CO to Pt. In other words, the increase in frequency of the Pt−C vibration upon negative-going potentials will slow down. Hence, a gradually decreasing Stark tuning rate for ν_{Pt-C} would be expected especially at largely negative potentials. This is consistent with the experimental observations (see Figure 3).

In the case of the CO intramolecular mode, the decrease in frequency of this band can also be explained in terms of greater charge flow from metal to CO $2\pi^*$ orbitals, which weakens the CO triple bond. This is in agreement with observation of the slope of 24 m^{-1}/V for ν_{CO} at −0.2 to 0.6 V. However, as mentioned above, this slope decreases rapidly at moderately negative potentials (near −0.2 V) and approaches almost zero at largely negative potentials. Apparently, the observation of almost constant frequency for ν_{CO} at potentials more negative than −1.0 V is not consistent with the corresponding greater π-back-donation from Pt to CO $2\pi^*$ orbitals. Although the cause of this potential-invariant properties of ν_{CO} frequency is still not clear now, the role of interfacial hydrogen ions, most possibly dissociated from the solvent formic acid, may not be ignored. The penetration of H^+ into the inner double layer may influence the distribution of interfacial fields, possibly weakening the electron density back-donated from Pt to CO molecules. Thus, the contradiction effect of H^+ to the electric field experienced by CO adlayers may slow down the decrease in frequency of ν_{CO} as the potential is altered to largely negative values. The potential-independent frequency properties of CO vibration were also found by Kim and co-workers[43] for CO on Pt in the hydrogen evolution region. More importantly, the present observation of nonlinear variation of frequency upon electrode potential, particularly that for ν_{Pt-C}, correlates well with the most recent quantum-chemical calculations based on density functional theory (DFT) by Weaver et al.[5] Using a finite cluster (Pt_{13}) method, they found that the Pt−C vibration of atop CO on Pt(111) reaches its maximum at about −1.4 V (relative to the zero-field potential, estimated from Figure 3 in ref 5), consistent with the present experimental results. Further examinations demonstrated a close correlation between the nonmonotonic field dependences for ν_{Pt-C} and the Pt−C bond distance, r_{Pt-CO}.

Despite that further vibrational data, obtained mainly in nonaqueous media for the ν_{Pt-C} and ν_{CO} vibration by SERS, are needed for insightful analysis of the nature of field-dependent chemisorbate bonding, some significant features can still be gleaned from the present experimental findings. The completely inverse trends for the Pt−C bond distance and corresponding frequency upon electric field (hence electrode potential) may reveal similar effects acting on them. The possible quantum chemical factors, including the steric repulsion and σ- and π-bonding as proposed by Weaver et al.,[5] would operate simultaneously in the field-induced changes in chemisorbate vibrational frequencies. The nearly offsetting contributions from the π-back-donation and σ-bonding along with the steric repulsion effect may be the main reason for observation of nearly potential-invariant frequency of ν_{Pt-C} at largely negative potentials. Apparently, similar comparison studies of both experimental and theoretical calculations of the Pt−CO system are worthy of broader attention in the future in order to obtain a better understanding of the field (potential)-dependent surface bonding.

Summary and Conclusions

We report in this work the potential-dependent surface-enhanced Raman spectra (SERS) of carbon monoxide adsorbed at the Pt−formic acid interface. Adsorbed carbon monoxide was exerted by dissociation of formic acid on platinum. To the best of our knowledge, it may be the first time to record the SERS spectra of CO adsorbed at a bare platinum surface in a nonaqueous medium. The use of nonaqueous solvent formic acid in the present study widened the potential window (about 3.0 V) available for detection of CO SERS features, in comparison with aqueous systems. The typical features observed at 475−490 and 2055−2080 cm^{-1}/V were assigned to the Pt−C and CO intramolecular vibration, respectively, indicating an atop adsorption model for CO on Pt. The bridging bonded CO was not confirmed in this study. Comparisons of the present data with previous studies in aqueous solutions show that solution components, particularly the dielectric in the inner double layer, may significantly influence the interaction of CO with platinum, especially the CO intramolecular mode. Electrooxidation of CO was observed to occur at potentials more positive than 0.6 V, being slightly negative relative to previous studies for CO on smooth platinum, suggestive of a higher electrocatalytic activity for the present highly roughened platinum surface.

The nonmonotonic field dependences of the ν_{Pt-C} and ν_{CO} vibration may be the key findings of the present study. This benefits mainly from the use of nonaqueous formic acid as solvent. The nonlinear tendency of frequency, especially that

for ν_{Pt-C}, was also predicted by a recent quantum-chemical calculation for CO on Pt(111), attributed mainly to the interplay of specific orbital and electrostatic interaction components. At positive and moderately negative potentials (−0.2 to 0.6 V), the Pt−C and CO intramolecular bands exhibit opposite frequency changes with decreasing potential, as normally observed in aqueous studies. As the potential is made more negative, the Stark tuning rate decreases rapidly, especially for ν_{CO}. The steric repulsion, σ-bonding, and π-back-donation may operate simultaneously to influence interaction of CO with platinum and hence the corresponding vibrational frequencies. In the case of ν_{Pt-C}, the nearly offsetting contributions from the π-back-donation and σ-bonding along with increasing steric repulsion from the negatively charged surface is reflected as observation of nearly potential-independent frequency properties for ν_{Pt-C} at largely negative potentials. While for ν_{CO}, π-back-donation may predominate at moderately negative potentials (−0.2 to 0.6 V), causing a continuous decrease in frequency. The rapid decrease in the Stark tuning rate for ν_{CO} at largely negative potentials (<-1.4 V) can be interpreted in terms of the gradual increase in concentration of H^+ in the inner double layer, which may weaken the electron density back-donated from Pt to CO molecules.

Acknowledgment. This work is supported by the Natural Science Foundation of China and the financial support of State Key Laboratory for Physical Chemistry of Solid Surfaces of Xiamen University. The Raman spectroscopy experiments were carried out in Xiamen University. The authors are grateful for the kind help of the co-workers there. A helpful discussion with Dr. Bin Ren is also greatly appreciated.

References and Notes

(1) Nichols, R. J. In *Adsorption of Molecules at Electrodes*; Lipkowski, J., Ross, P. N., Eds.; VCH: New York, 1992; Chapter 7.

(2) Ren, B.; Li, X. Q.; She, C. X.; Wu, D. Y.; Tian, Z. Q. *Electrochim. Acta* **2000**, *46*, 193. (b) Tian, Z. Q.; Ren, B.; Mao, B. W. *J. Phys. Chem. B* **1997**, *101*, 1338.

(3) Zheng, M. S.; Sun, S. G. *J. Electroanal. Chem.* **2001**, *500*, 223. (b) Sun, S. G. In *Electrocatalysis*; Lipkowski, J., Ross, P. N., Eds.; Wiley-VCH: New York, 1998; p 243.

(4) Thomas, V. D.; Schwank, J. W.; Gland, J. L. *Surf. Sci.* **2000**, *464*, 153.

(5) Wasileski, S. A.; Weaver, M. J.; Koper, M. T. M. *J. Electroanal. Chem.* **2001**, *500*, 344.

(6) Villegas, I.; Weaver, M. J. *J. Phys. Chem. B* **1997**, *101*, 10166.

(7) Dellwig, T.; Hartmann, J.; Libuda, J.; Meusel, I.; Rupprechter, G.; Unterhalt, H.; Freund, H.-J. *J. Mol. Catal. A: Chem.* **2000**, *162*, 51.

(8) Rupprechter, G.; Unterhalt, H.; Morkel, M.; Galletto, P.; Hu, L.; Freund, H.-J. *Surf. Sci.* **2002**, *502*−*503*, 109.

(9) Brandt, R. K.; Sorbello, R. S.; Greenler, R. G. *Surf. Sci.* **1992**, *271*, 605.

(10) Nanbu, N.; Kitamura, F.; Ohsaka, T.; Tokuda, K. *J. Electroanal. Chem.* **2000**, *485*, 128.

(11) Loster, M.; Friedrich, K. A. *Surf. Sci.* **2003**, *523*, 287.

(12) Kung, K. Y.; Chen, P.; Wei, F.; Shen, Y. R.; Somorjai, G. A. *Surf. Sci.* **2000**, *463*, L627.

(13) Vidal, F.; Busson, B.; Six, C.; Pluchery, O.; Tadjeddine, A. *Surf. Sci.* **2002**, *502*−*503*, 485.

(14) Condon, E. U. *Phys. Rev.* **1932**, *41*, 759. For recent reviews, see: (a) Lambert, D. K. *Solid State Commun.* **1984**, *51*, 297. (b) Holloway, S.; Norskov, J. K. *J. Electroanal. Chem.* **1984**, *161*, 193. (c) Korzeniewski, C.; Shirts, R. B.; Pons, S. *J. Phys. Chem.* **1985**, *89*, 2297. (d) Zou, S.; Weaver, M. J. *J. Phys. Chem.* **1996**, *100*, 4237. (e) Wasileski, S. A.; Koper, M. T. M.; Weaver, M. J. *J. Am. Chem. Soc.* **2002**, *124*, 2796.

(15) Lambert, D. K. *Electrochim. Acta* **1996**, *41*, 623.

(16) Weaver, M. J.; Zou, S. In *Spectroscopy for Surface Science Advances in Spectroscopy*; Clark, R. J. H., Hester, R. E., Eds.; Wiley: Chichester, 1998; Vol. 26, Chapter 5.

(17) Leung, L. W. H.; Weaver, M. J. *J. Am. Chem. Soc.* **1987**, *109*, 5113.

(18) Zou, S.; Weaver, M. J. *Anal. Chem.* **1998**, *70*, 2387.

(19) Cao, P. G.; Yao, J. L.; Ren, B.; Gu, R. A.; Tian, Z. Q. *Chem. Phys. Lett.* **2000**, *316*, 1.

(20) Tian, Z. Q.; Ren, B.; Wu, D. Y. *J. Phys. Chem. B* **2002**, *106*, 9463.

(21) Cao, P. G.; Yao, J. L.; Ren, B.; Gu, R. A.; Tian, Z. Q. *J. Phys. Chem. B* **2002**, *106*, 7283.

(22) Cao, P. G.; Gu, R. A.; Ren, B.; Tian, Z. Q. *Chem. Phys. Lett.* **2002**, *366*, 440.

(23) Huang, J. M.; Korzeniewski, C. *J. Electroanal. Chem.* **1999**, *471*, 146.

(24) Anderson, M. R.; Blackwood, D.; Pons, S. *J. Electroanal. Chem.* **1988**, *256*, 387.

(25) Anderson, M. R.; Blackwood, D.; Richmond, T. G.; Pons, S. *J. Electroanal. Chem.* **1988**, *256*, 397.

(26) Beden, B.; Bewick, A.; Lamy, C. *J. Electroanal. Chem.* **1983**, *150*, 505.

(27) Kunimatsu, K.; Kita, H. *J. Electroanal. Chem.* **1987**, *218*, 155.

(28) Watanabe, N.; Iwatsu, K.; Yamakata, A.; Ohtani, T.; Kubota, J.; Kondo, J. N.; Wada, A.; Domen, K.; Hirose, C. *Surf. Sci.* **1996**, *368*, 270.

(29) Cao, P. G.; Sun, Y. H.; Gu, R. A. *J. Phys. Chem. B*, to be submitted.

(30) Mrozek, M. F.; Luo, H.; Weaver, M. J. *Langmuir* **2000**, *16*, 8463. (b) Weaver, M. J. *J. Raman Spectrosc.* **2002**, *33*, 309.

(31) Cai, W. B.; Ren, B.; Li, X. Q.; She, C. X.; Liu, F. M.; Cai, X. W.; Tian, Z. Q. *Surf. Sci.* **1998**, *406*, 9.

(32) Zhang, Y.; Weaver, M. J. *Langmuir* **1993**, *9*, 1397.

(33) Kizhakevariam, N.; Villegas, I.; Weaver, M. J. *Langmuir* **1995**, *11*, 2777. (b) Baro, A. M.; Ibach, H. *J. Chem. Phys.* **1979**, *71*, 4812.

(34) Sheppard, N.; Nguyen, T. T. In *Advances in Infrared and Raman Spectroscopy*; Clark, R. J. H., Hester, R. E., Eds.; Heyden: London, 1978; Vol. 5, p 67.

(35) Li, X. Q. M.Sc. Thesis, Xiamen University, 1998; Chapter 3.

(36) Kunimatsu, K.; Shimazu, K.; Kita, H. *J. Electroanal. Chem.* **1988**, *256*, 371.

(37) Anderson, M. R.; Huang, J. *J. Electroanal. Chem.* **1991**, *318*, 335. (b) Roth, J. D.; Weaver, M. J. *Langmuir* **1992**, *8*, 1451. (c) Roth, J. D.; Chang, S. C.; Weaver, M. J. *J. Electroanal. Chem.* **1990**, *288*, 285.

(38) Blyholder, G. *J. Phys. Chem.* **1964**, *68*, 2772.

(39) Pacchioni, G.; Koutecky, J. *J. Phys. Chem.* **1987**, *91*, 2658. (b) Hermann, K.; Bagus, P. S.; nelin, C. J. *Phys. Rev. B* **1987**, *35*, 9467. (c) Ricart, J. M.; Rubio, J.; Illas, F.; Bagus, P. S. *Surf. Sci.* **1994**, *304*, 335.

(40) Love, J. G.; McQuillan, A. J. *J. Electroanal. Chem.* **1989**, *274*, 263.

(41) Korzeniewski, C.; Pons, S.; Schmidt, P. P.; Severson, M. W. *J. Chem. Phys.* **1986**, *85*, 4153.

(42) Head-Gordon, M.; Tully, J. C. *Chem. Phys.* **1993**, *175*, 37.

(43) Kim. C. S.; Tornquist, W. J.; Korzeniewski, C. *J. Phys. Chem.* **1993**, *97*, 6484.